DESY 05-045

arXiv:hep-ph/0505024 v1 4 May 2005

DESY 05-045

HOW TO DETECT BIG BANG RELIC NEUTRINOS?[a]

Andreas Ringwald
Deutsches Elektronen-Synchrotron DESY
Notkestraße 85, D–22607 Hamburg, Germany
E-mail: Andreas.Ringwald@desy.de

ABSTRACT

The existence of big bang relic neutrinos—exact analogues of the big bang relic photons comprising the cosmic microwave background radiation—is a basic prediction of standard cosmology. At present, the observational evidence for their existence rests entirely on cosmological measurements, such as the light elemental abundances, anisotropies in the cosmic microwave background, and the large-scale matter power spectrum. In this review, we concentrate on the prospects of more direct, weak interaction based relic neutrino detection techniques which are sensitive to the cosmic neutrino background near the present epoch and in our local neighborhood in the universe. In this connection, we emphasize the necessity to take into account the gravitational clustering of the relic neutrinos in the cold dark matter halos of our Milky Way and nearby galaxy clusters.

1. Introduction

Over the last few years, significant advances were made in observational cosmology[1)]. The position of the first Doppler peak in recent measurements of the cosmic microwave background (CMB) radiation strongly suggests that the universe is spatially flat. Observations of Type Ia supernovae (SN) and the large scale structure (LSS) favor a universe with present energy fractions of 70 % of dark energy—accounting for the observed accelerating expansion of the universe—and about 25 % of cold dark matter—the corresponding particles being non-relativistic already at the time of recombination. Successful big-bang nucleosynthesis (BBN) of the light elements requires that about 5 % of the energy content of the universe is in the form of ordinary baryonic matter. All in all, we have now a pretty good knowledge of the cosmic recipe (cf. Table 1). A lot of further observational and theoretical effort will go into this field to further substantiate and explain these cosmological findings, and, in particular, to clarify the nature of dark energy and dark matter.

Along with the CMB, standard big bang theory predicts the existence of a cosmic neutrino background (CνB). Presently, the evidence for the existence of the relic neutrinos rests on the aforementioned cosmological measurements, i.e. the light elemental abundances, CMB anisotropies, and the large-scale matter power spectrum[2,3)]. Note,

[a] Talk at XI International Workshop on "Neutrino Telescopes", Feb 22-25, 2005, Venice, Italy.

Table 1: The cosmic recipe.

Material	Particles	$\langle E \rangle$ or m	N	$\langle \rho \rangle / \rho_c$	Obs. Evid.
Radiation	γ	0.1 meV	10^{87}	0.01 %	CMB
Hot Dark Matter	Neutrinos	> 0.04 eV < 0.6 eV	10^{87}	> 0.1 % < 2 %	BBN CMB LSS
Ordinary Matter	p, n, e	MeV-GeV	10^{78}	5 %	BBN CMB
Cold Dark Matter	WIMPs? Axions?	$\gtrsim 100$ GeV $\lesssim$ meV	$\lesssim 10^{77}$ $\gtrsim 10^{91}$	25 %	LSS CMB
Dark Energy	?	10^{-33} eV	?	70 %	SN CMB

however, that all these measurements probe only the presence of the relic neutrinos at early stages in the cosmological evolution, and this often in a rather indirect way. It is therefore natural to ask: what are the prospects of a more direct, weak interaction based relic neutrino detection, sensitive in particular to the CνB in the present epoch[4)]? After all, among the known elementary particles, neutrinos are one of the most abundant particles in the present universe, falling second only to the relic photons (cf. Table 1).

2. How Many? How Fast?

In order to design a direct, weak interaction based detection experiment, a precise knowledge of the phase space distribution of the relic neutrinos is indispensable. In this section, we will review recent determinations of this distribution[5,6)].

The big bang relic neutrinos originate from the decoupling of the weak interactions when the universe was about one second old and the primordial plasma had a temperature of about one MeV, much larger than the possible neutrino masses. Neglecting late-time, small-scale gravitational clustering, to which we come later, and in the absence of appreciable lepton asymmetries,[b] their phase space distribution is therefore predicted to be given by the homogenous and isotropic relativistic Fermi-Dirac distribution, $f_0(p) = 1/(1 + \exp(p/T_{\nu,0}))$, where p is the modulus of the comoving three-momentum $\mathbf{p}$ and $T_{\nu,0} = (4/11)^{1/3}\, T_{\gamma,0} = 1.95$ K is today's neutrino temperature. Correspondingly, the gross properties of the CνB are tightly related to

[b] Large neutrino mixing inferred from oscillation experiments ensures the validity of the neglection of chemical potentials[7,8,9,10)].

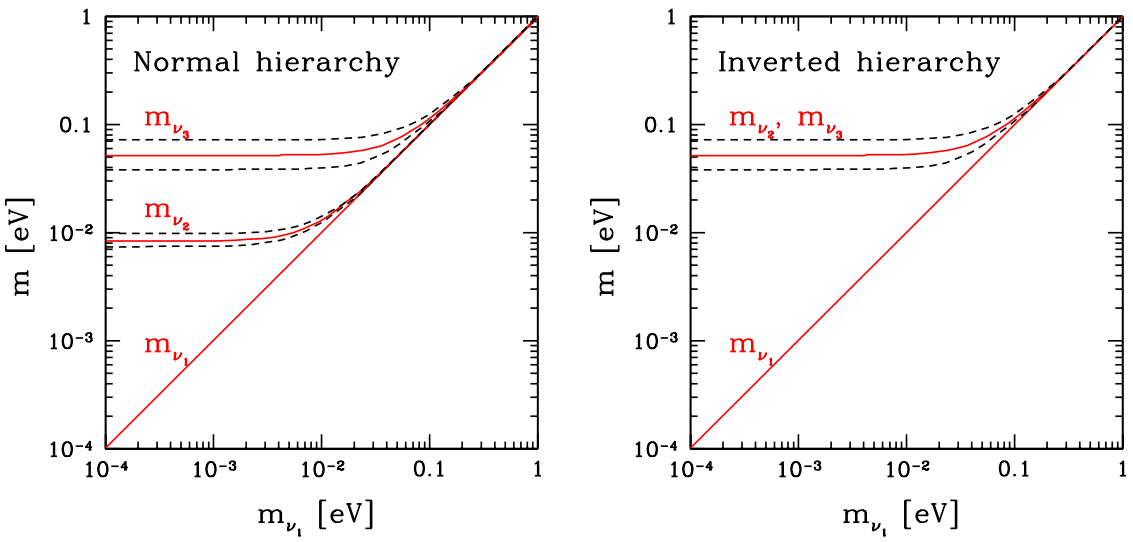

Figure 1: Present knowledge about the neutrino mass spectrum[11], as a function of the mass of the lightest neutrino, m_{ν_1}. In the normal hierarchical spectrum (left), the smaller mass difference inferred from solar neutrino oscillations separates the lightest neutrino from the next-to-lightest, whereas the larger mass difference inferred from atmospheric neutrino oscillations separates the latter from the heaviest neutrino. In the inverted hierarchical spectrum (right) this is reversed.

the properties of the well-measured CMB and are therefore to be considered as rather firm predictions. Their present number density,

$$\underbrace{\bar{n}_{\nu_i\,0} = \bar{n}_{\bar{\nu}_i\,0}}_{\mathrm{C}\nu\mathrm{B}} = \frac{3}{22}\,\underbrace{\bar{n}_{\gamma\,0}}_{\mathrm{CMB}} = 56\ \mathrm{cm}^{-3}\,, \tag{1}$$

when summed over all neutrino types $i = 1, 2, 3$, is large and comparable to the one of the CMB, $\sum_i(\bar{n}_{\nu_i\,0} + \bar{n}_{\bar{\nu}_i\,0}) = (9/11)\,\bar{n}_{\gamma\,0}$. Their present average three-momentum, on the other hand, is very small,

$$\underbrace{\bar{p}_{\nu_i\,0} = \bar{p}_{\bar{\nu}_i\,0}}_{\mathrm{C}\nu\mathrm{B}} = 3\,(\frac{4}{11})^{1/3}\,\underbrace{T_{\gamma\,0}}_{\mathrm{CMB}} = 5\times 10^{-4}\ \mathrm{eV}\,. \tag{2}$$

Correspondingly, at least two of the relic neutrino mass eigenstates are non-relativistic today ($m_{\nu_i} \gg \bar{p}_{\nu_i\,0}$), independently of whether neutrinos masses have a normal hierarchical or inverted hierarchical pattern (cf. Fig. 1). These neutrinos are subject to gravitational clustering into gravitational potential wells due to existing CDM and baryonic structures, possibly causing the local neutrino number density to be enhanced relative to the standard value (1) and the momentum distribution to deviate from the relativistic Fermi-Dirac distribution.

This question can be studied quantitatively as follows[5,6]. First of all, in the context of a flat ΛCDM model, the neutrino contribution to the total dark matter

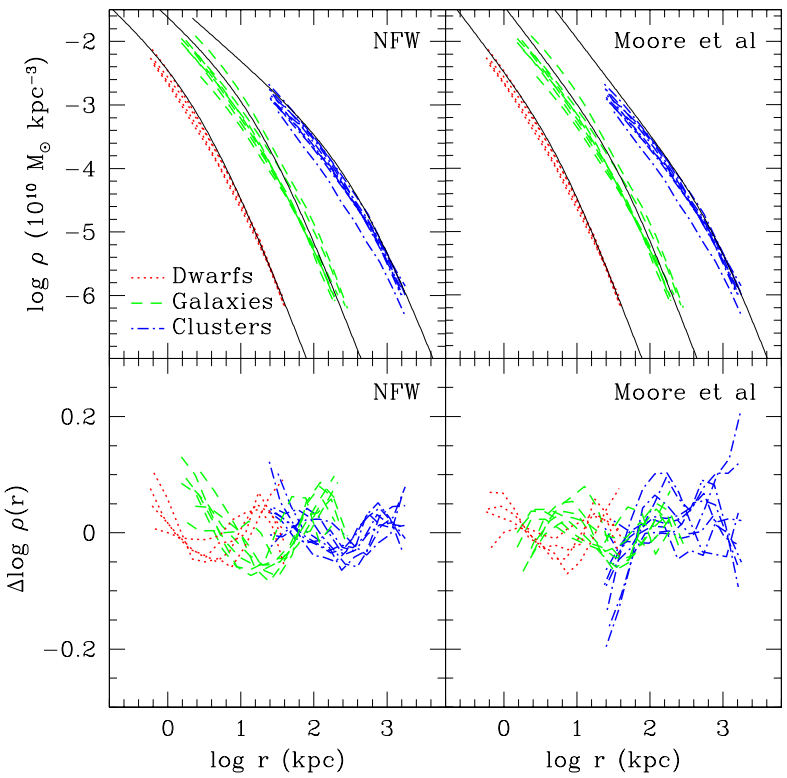

Figure 2: CDM mass density profiles inferred from N-body simulations of ΛCDM models[12].

density is always a small perturbation (cf. Table 1). Correspondingly, the CDM mass density ρ_m dominates in the gravitational potential ϕ. Secondly, the neutrinos will have negligible gravitational interactions with each other. Therefore, one can make use of the CDM halo profiles from high-quality, pure ΛCDM simulations (cf. Fig. 2) and study the evolution of the neutrino phase space distribution $f_{\nu_i}(\mathbf{x}, \mathbf{p}, \tau)$ in the corresponding gravitational potential wells. This distribution depends on the comoving distance $\mathbf{x} = \mathbf{r}/a(t)$, its conjugate momentum $\mathbf{p} = a m_{\nu_i} \dot{\mathbf{x}}$, and the conformal time $d\tau = dt/a(t)$, a being the cosmological scale factor. Technically speaking, one has then to solve the Vlasov, or collisionless Boltzmann equation,

$$\frac{D f_{\nu_i}}{D\tau} \equiv \frac{\partial f_{\nu_i}}{\partial \tau} + \dot{\mathbf{x}} \cdot \frac{\partial f_{\nu_i}}{\partial \mathbf{x}} \underbrace{-a m_{\nu_i} \nabla \phi}_{\dot{\mathbf{p}}} \cdot \frac{\partial f_{\nu_i}}{\partial \mathbf{p}} = 0 \,, \tag{3}$$

with the Poisson equation

$$\nabla^2 \phi = 4\pi G a^2 \underbrace{\left(\rho_m(\mathbf{x}, \tau) - \overline{\rho}_m(\tau)\right)}_{\delta_m(\mathbf{x},\tau)\overline{\rho}_m(\tau)} \tag{4}$$

relating the gravitational potential ϕ to the CDM density fluctuation δ_m with respect to the physical mean $\bar{\rho}_m$. For a given CDM halo profile, e.g. the one advocated by

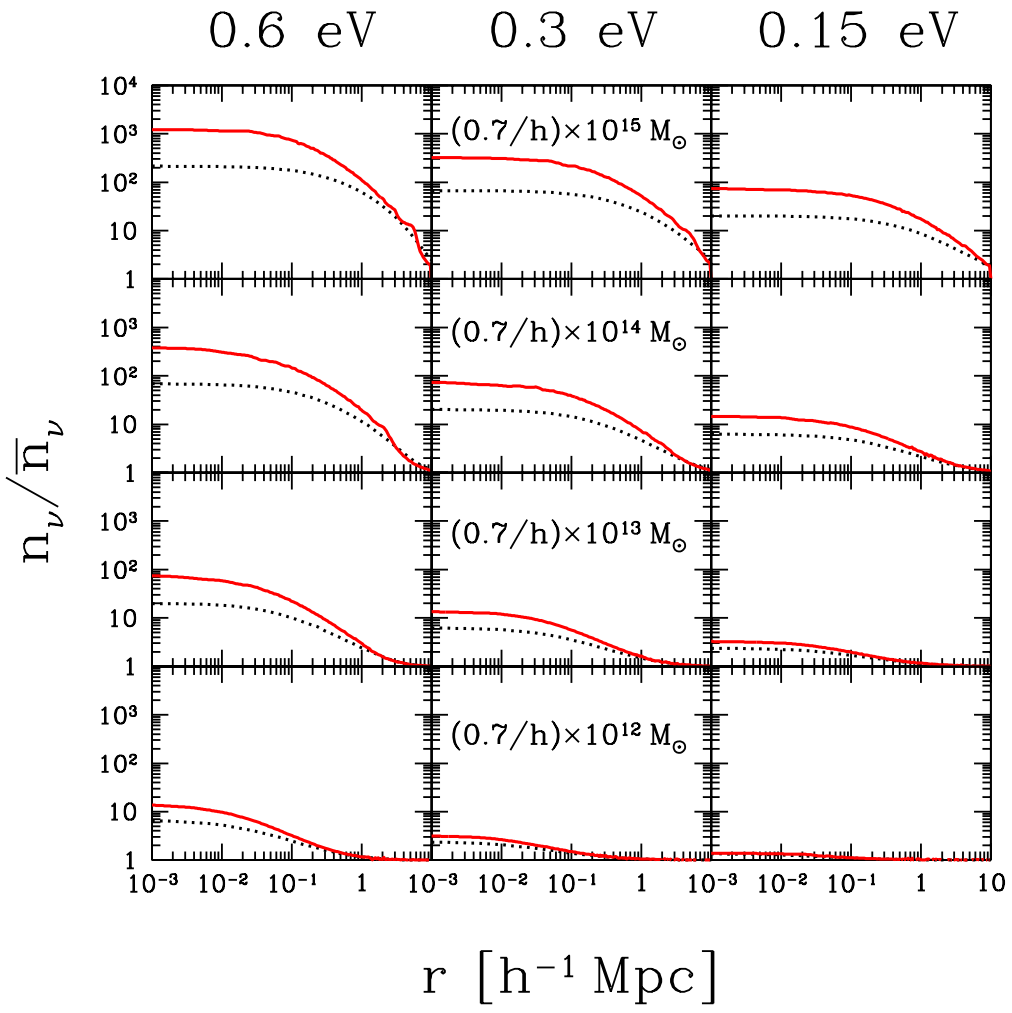

Figure 3: Neutrino number density profiles, normalized to their cosmological mean[6], calculated with N-one-body simulations (solid) and with the linear approximation (dotted), respectively.

Navarro, Frenk, and White (NFW)[13,14],

$$\rho_m(r) = \frac{\rho_s}{(r/r_s)(1+r/r_s)^2}\,, \tag{5}$$

where the parameters r_s and ρ_s are basically determined by the halo's virial mass $M_{\rm vir}$, the Vlasov equation (3) may be solved numerically by tracking the trajectories of neutrinos in phase space, starting from initial conditions corresponding to the homogeneous and isotropic Fermi-Dirac distribution (N-one-body simulations)[6]. The initial redshift can be taken as $z = 3$, since, at higher redshifts, a sub-eV neutrino has too much thermal velocity to cluster efficiently.

A comprensive and exhaustive comparative study[6] has revealed the following results (cf. Fig. 3). First of all, a flattening of the neutrino profiles at small radii is

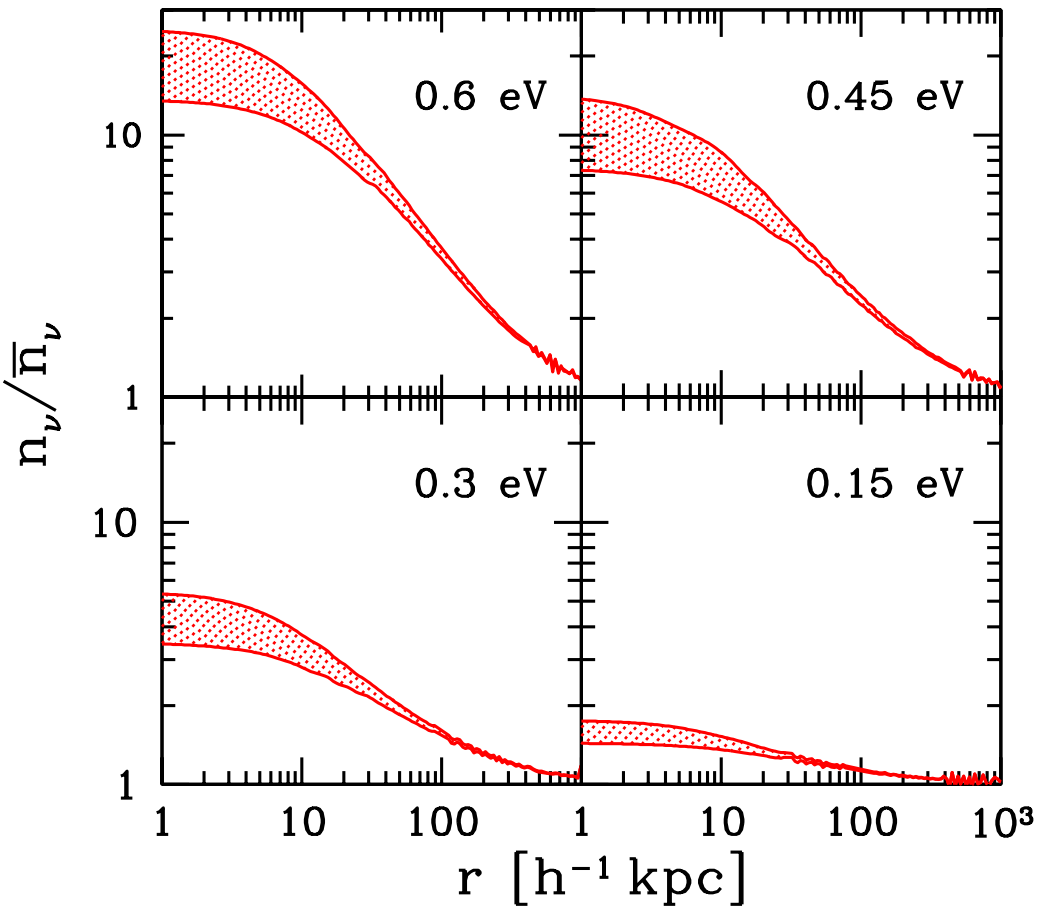

Figure 4: Neutrino density profiles for the Milky Way[6], obtained via N-one-body simulations from the MWnow (top curve in each plot) and the NFWhalo run (bottom curve in each plot).

observed, in distinction to the CDM profiles (cf. Fig. 2)). This can be understood in terms of neutrino free-streaming. Secondly, the clustering is considerably improved towards larger CDM halo virial masses and/or larger neutrino masses. In the inner part ($\lesssim$100 kpc) of a massive galaxy cluster like e.g. the nearby ($\sim$ 15 Mpc) Virgo cluster ($M_{\rm vir} \sim 10^{15}\, M_\odot$), the relic neutrino density n_ν can be larger than its cosmological mean $\bar{n}_\nu$ by a factor of $\sim 10 \div 1000$, if we take into account the full range of possible neutrino masses for the heaviest neutrinos, $m_\nu = 0.04 \div 0.6$ eV (cf. Fig. 1). Much more moderate clustering, $n_\nu/\bar{n}_\nu \sim 1 \div 20$, is obtained for ordinary galaxies like the Milky Way ($M_{\rm vir} \sim 10^{12}\, M_\odot$) in their central region ($\lesssim$10 kpc). We note in passing that a previously[5] exploited semi-analytical linear method for solving the Vlasov equation (3), which consists of replacing $\partial f/\partial \mathbf{p}$ by $\partial f_0/\partial \mathbf{p}$, systematically underestimates the neutrino overdensities over nearly the whole range of halo and neutrino masses considered here (cf. Fig. 3).

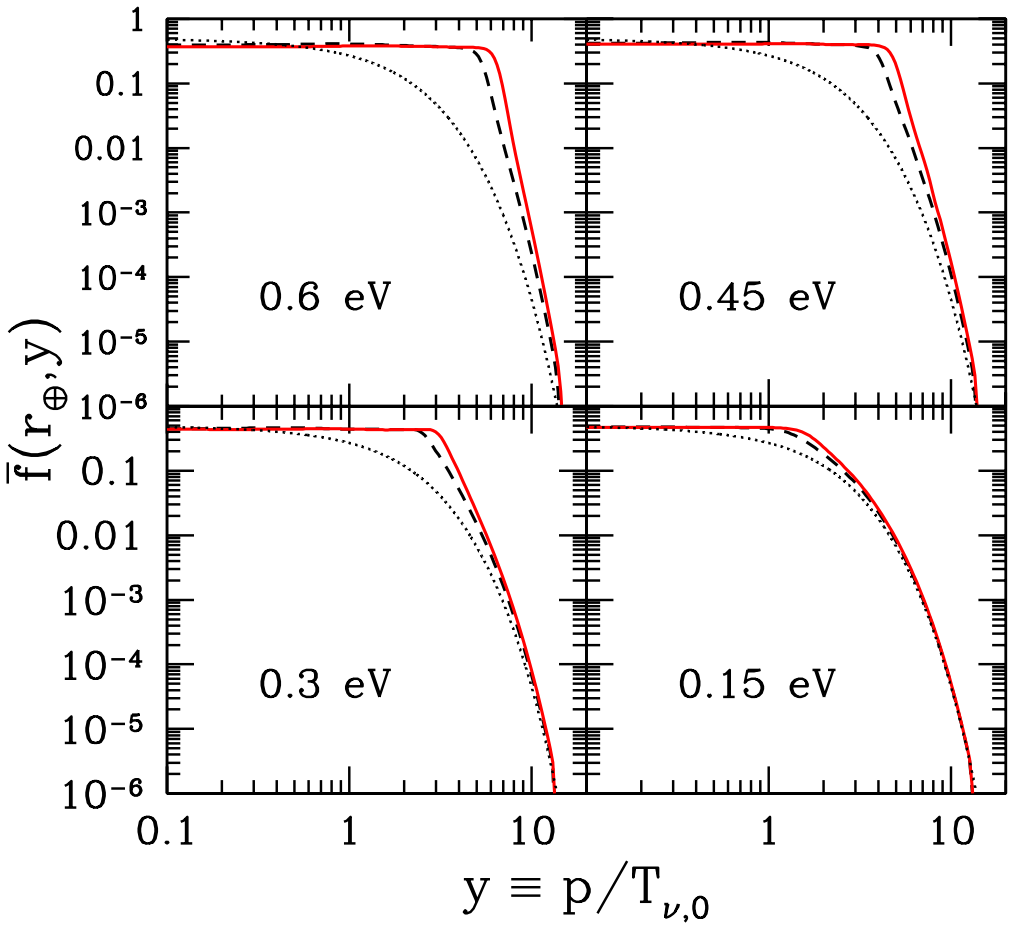

Figure 5: Momentum distribution of the relic neutrinos in the local neighbourhood of the Earth[6], obtained from the MWnow (solid) and NFWhalo (dashed) run, approaching for large momenta the relativistic Fermi-Dirac distribution (dotted).

For an accurate determination of the relic neutrino number density and momentum distribution in the Earth's local neighbourhood in the Milky Way, at a distance $r_\oplus \sim 8$ kpc from the galactic center, one needs, in principle, to know the gravitational potential over the history of the Milky Way, i.e. the complete assembly history. In the absence of that information, one may consider two extreme cases, with the true behavior somehow lying in-between: (i) working with the present day Milky Way mass distribution[15,16] (MWnow), assuming it to be static (in physical coordinates), and (ii) exploiting the NFW halo (NFWhalo) that would have been there, had baryon compression—which is thought to lead to the formation of the galactic bulge and disk—not taken place. The possible ranges of overdensities, $\sim 1 \div 20$, in the Milky Way are illustrated in Fig. 4.

The final momentum distribution at $r_\oplus$ is found to be almost isotropic, with mean radial velocity $\langle v_r \rangle \approx 0$ and second moments that satisfy approximately the relation

Table 2: Relic neutrino properties[6] as relevant for flux detection.

	$\frac{n_\nu}{\bar{n}_\nu}$	$\lambda\!\!\!^{-} = \frac{1}{\langle p \rangle}$	$\langle v \rangle$
MWnow $m_\nu =$			
0.6 eV	20	2.3×10^{-2} cm	1.4×10^{-3}
0.45 eV	10	2.9×10^{-2} cm	1.5×10^{-3}
0.3 eV	4.4	3.7×10^{-2} cm	1.8×10^{-3}
0.15 eV	1.6	4.1×10^{-2} cm	3.2×10^{-3}
NFWhalo $m_\nu =$			
0.6 eV	12	2.7×10^{-2} cm	1.2×10^{-3}
0.45 eV	6.4	3.4×10^{-2} cm	1.3×10^{-3}
0.3 eV	3.1	3.9×10^{-2} cm	1.7×10^{-3}
0.15 eV	1.4	5.9×10^{-2} cm	2.2×10^{-3}

$2\langle v_r^2 \rangle \approx \langle v_T^2 \rangle$. The coarse-grained phase space densities $\bar{f}(r_\oplus, p)$ in Fig. 5 are flat at low momenta, with a common value of nearly $1/2$, have a turning point at about the escape momenta $p_{\rm esc} \equiv m_\nu v_{\rm esc} \equiv m_\nu \sqrt{2|\phi(r_\oplus)|}$, and quickly approach the Fermi-Dirac distribution for larger momenta. Note, that the results displayed in Fig. 5 not only satisfy, but, up to $p_{\rm esc}$, nearly completely saturate the general phase space bound[17,18] $\bar{f} \leq \max(f_0) = 1/2$. The corresponding semi-degenerate state can only be made denser by filling in states above $p_{\rm esc}$. In order to attain even higher densities, one must appeal to non-standard theories[19].

3. How to Detect?

The gravitational infall of the relic neutrinos into CDM halos, discussed in the last section, might be significant for its influence on the non-linear (i.e. not so large-scale, wave number $k \gtrsim 1$ Mpc^{-1}) matter power spectrum[20,21], which will be determined in the upcoming weak gravitational lensing campaigns. In contrast to the evidences for the relic neutrinos from BBN, CMB, and the linear (i.e. large-scale, $k \lesssim 1$ Mpc^{-1}) matter power spectrum mentioned in the Introduction, this gravitational inference will test the presence of relic neutrinos at low redshift, i.e. near to the present epoch. In this section, we will concentrate on other detection techniques, which are also sensitive to the present CνB, which, however, are based instead on weak interaction scattering processes involving the relic neutrinos either as a beam or as a target[6].

3.1. Flux detection

The Earth is moving through the almost isotropic (cf. last section) relic neutrino background. In this subsection, we consider coherent elastic scattering of the

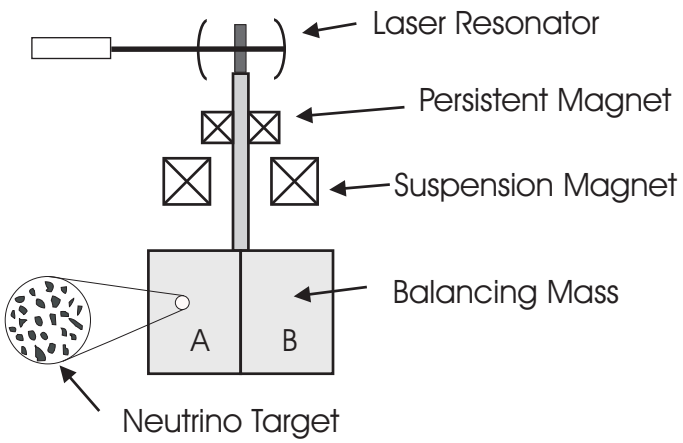

Figure 6: Cavendish-type torsion balance for relic neutrino detection[25,26].

corresponding relic neutrino flux off target matter in a terrestrial detector. In this connection, it is an important observation that the low average momentum of relic neutrinos corresponds to a de Broglie wavelength of macroscopic dimension,

$$\lambda\!\!\!^{-} = 1/\langle p \rangle = 0.12 \;\; \mathrm{cm}/\langle p/T_{\nu,0} \rangle \, . \tag{6}$$

Correspondingly, one may envisage[22,23] scattering processes in which many target atoms of atomic mass A act coherently over a macroscopic volume $\lambda\!\!\!^{-3}$, yielding an enhancement of the elastic scattering rate by the huge factor

$$\frac{N_A}{A}\,\rho_{\rm t}\,\lambda\!\!\!^{-3} \simeq 6 \times 10^{18} \left(\frac{100}{A}\right) \left(\frac{\rho_{\rm t}}{\mathrm{g/cm^3}}\right) \left(\frac{\lambda\!\!\!^{-}}{0.1 \;\mathrm{cm}}\right)^3 \, , \tag{7}$$

where N_A is Avogadro's number and $\rho_{\rm t}$ is the target mass density, compared to case where neutrinos are elastically scattered coherently only on the individual nuclei of the target. A terrestrial target of linear size $r_{\rm t} < \lambda\!\!\!^{-}$ will therefore experience a neutrino wind induced acceleration[22,23,24]

$$\begin{aligned} a_{\rm t} \;&\simeq\; \sum_{\nu,\bar\nu} \underbrace{n_\nu \, v_{\rm rel}}_{\rm flux} \, \frac{4\pi}{3} \, N_A^2 \, \rho_{\rm t} \, r_{\rm t}^3 \, \sigma_{\nu N} \, \underbrace{2\, m_\nu \, v_{\rm rel}}_{\rm mom.\,transfer} \\ &\simeq\; 2 \times 10^{-28} \; \frac{\rm cm}{\rm s^2} \left(\frac{n_\nu}{\bar n_\nu}\right) \left(\frac{10^{-3}\, c}{v_{\rm rel}}\right) \left(\frac{\rho_{\rm t}}{\mathrm{g/cm^3}}\right) \left(\frac{r_{\rm t}}{\lambda\!\!\!^{-}}\right)^3 \, , \end{aligned} \tag{8}$$

where $\sigma_{\nu N} \simeq G_F^2 \, m_\nu^2/\pi$ is the elastic neutrino–nucleon cross section, and $v_{\rm rel} = \langle |\mathbf{v} - \mathbf{v}_\oplus| \rangle$ is the mean velocity of the relic neutrinos in the rest system of the detector. Here, $v_\oplus \simeq 7.7 \times 10^{-4}\, c$ denotes the velocity of the Earth through the Milky Way. For Majorana neutrinos, the acceleration is further suppressed, in comparison with (8), by a factor of $(v_{\rm rel}/c)^2 \simeq 10^{-6}$ for an unpolarized and $v_{\rm rel}/c \simeq 10^{-3}$ for a polarized target, respectively.

Table 3: Planned and projected accelerator beams and their interaction rates with the relic neutrinos[6].

accel.	N	E_N [TeV]	L [km]	I [A]	$\frac{R_{\nu A}}{\left[\frac{n_\nu}{\bar{n}_\nu}\,\frac{m_\nu}{\mathrm{eV}}\right]}$ [yr^{-1}]
LHC	p	7	26.7	0.6	2×10^{-8}
	Pb	574	26.7	0.006	1×10^{-5}
VLHC	p	87.5	233	0.06	2×10^{-7}
	Pb	7280	233	0.0006	1×10^{-4}
ULHC	p	10^7	40 000	0.1	10

What are the prospects to measure such small accelerations? Presently, conventional Cavendish-type torsion balances routinely reach 10^{-13} cm s^{-2}. Possible improvements with currently available technology to a sensitivity of $\gtrsim 10^{-23}$ cm s^{-2} have been proposed[25,26] (cf. Fig. 6)[c]. However, even such an improved sensitivity is still off the prediction (8) by at least three orders of magnitude, as an inspection of the currently allowed range of local relic neutrino overdensities in Table 2 reveals. Therefore, an observation of this effect will not be possible within the upcoming decade. But it can still be envisaged in the not-so-distant future, say, within thirty to forty years. Note, in this context, that the acceleration (8) can be improved still by a considerable amount by using foam-like[22] or laminated[23] materials. In this way one may exploit a target size much larger than $\lambda\!\!\!^{-}$, while still avoiding destructive interference. Alternatively, grains of size $\sim \lambda\!\!\!^{-}$ could be randomly embedded (with spacing $\sim \lambda\!\!\!^{-}$) in a low density host material[27,28]. Advances in nanotechnology may be very welcome in this connection. For the case of Majorana neutrinos, flux detection via mechanical forces will remain a real challenge, however.

3.2. Target detection

The weak interaction cross sections are rapidly growing with energy, at least at center-of-mass energies below the W- and Z-resonances. In this subsection, we study the question whether the scattering of extremely energetic particles (accelerator beams or cosmic rays) off the relic neutrinos as a target has promising prospects for CνB detection.

[c] Such improvements would also be very interesting in the connection of the search for deviations from Newton's law at small distances and possible significant improvements on the bounds of the size of extra space-like dimensions[1].

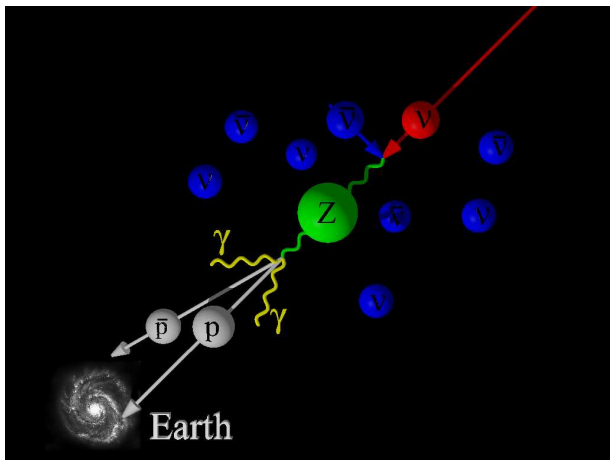

Figure 7: Resonant annihilation of an extremely energetic cosmic neutrino off a relic anti-neutrino into a Z-boson[33].

3.2.1. Exploiting accelerator beams

For a beam of particles ${}^{A}_{Z}N$, with energy E_N, charge $Z\,e$, length L, and current I, the interaction rate with the relic neutrinos is of order[29,30,31]

$$\begin{aligned} R_{\nu\,{}^{A}_{Z}N} &\simeq \sum_{\nu,\bar{\nu}} n_\nu\,\sigma_{\nu\,{}^{A}_{Z}N}\,L\;I/(Z\,e) \qquad (9)\\ &\simeq 2\times 10^{-8}\ \mathrm{yr}^{-1}\ \left(\frac{n_\nu}{\bar{n}_\nu}\right)\left(\frac{m_\nu}{\mathrm{eV}}\right)\frac{A^2}{Z}\ \left(\frac{E_N}{10\ \mathrm{TeV}}\right)\left(\frac{L}{100\ \mathrm{km}}\right)\left(\frac{I}{0.1\ \mathrm{A}}\right)\,. \end{aligned}$$

In view of the currently allowed range of local relic neutrino overdensities, $\sim 1 \div 20$, and the beam parameters of the next and next-to-next generation of accelerators—the Large Hadron Collider (LHC) and the Very Large Hadron Collider (VLHC), respectively—the expected rate (9) is clearly too small to give rise to an observable effect in the foreseeable future (cf. Table 3). Even with an Ultimate Large Hadron Collider (ULHC) designed to accelerate protons to energies above 10^7 TeV in a ring of ultimate circumference $L \simeq 4\times 10^4$ km around the Earth,[d] it seems very difficult to establish the interactions with the relic neutrinos, although they occur at a rate of more than one event per year (cf. Table 3): elastic scattering of the beam particles with the relic neutrinos—one of the contributions to the rate (9)—will be next to impossible to detect because of the small momentum transfers involved (~ 1 GeV at

[d] Note that such an accelerator, in the collider mode, will probe the "intermediate" scale $(M_{\mathrm{EW}}\,M_{\mathrm{GUT}})^{1/2} \sim 10^{10}$ GeV between the electroweak scale $M_{\mathrm{EW}} \sim 1$ TeV and the scale of grand unification $M_{\mathrm{GUT}} \sim 10^{17}$ GeV. The intermediate scale is exploited in many schemes of supersymmetry breaking and in seesaw mechanisms for neutrino masses.

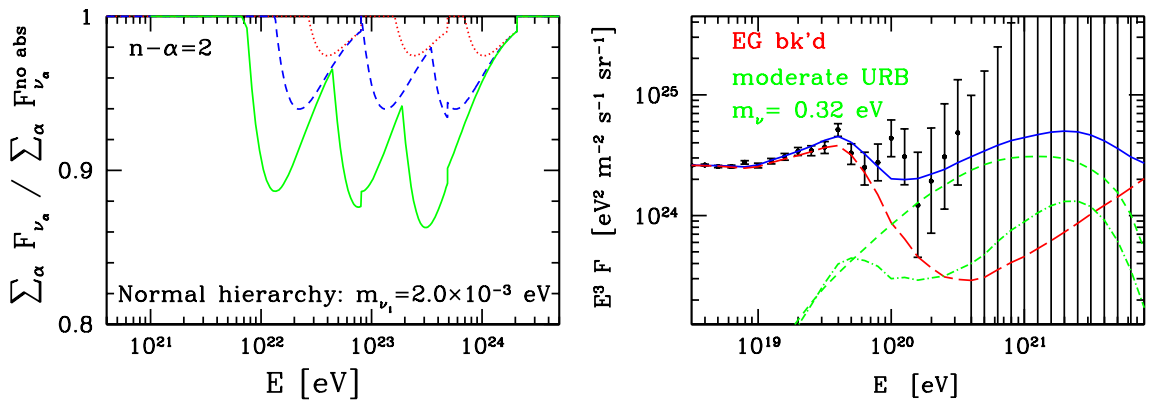

Figure 8: Signatures of resonant annihilation of extremely energetic cosmic neutrinos off relic neutrinos: absorption dips (left) in the EECν flux[11], for an isotropic source distribution out to redshift $z_{\max} = 2, 5, 10$ (from upper to lower curves), and emission features (Z-bursts) (right) in the EEC ray (EECR) flux[44] flux in the form of photons (short-dashed) and protons (dashed-dotted), eventually overcoming the ordinary extragalactic EECR flux (long dashed), which suffers from the GZK cutoff.

$E_N \sim 10^7$ TeV). A very promising alternative is to consider a heavy ion beam, and to exploit the contribution of the inverse beta decay reaction,

$$ {}^{A}_{Z}N + \nu_e \to {}^{A}_{Z+1}N + e^- \,, \tag{10} $$

to the rate (9). This reaction changes the charge of the nucleus, causing it to follow an extraordinary trajectory and finally to exit the machine such that it becomes susceptible to detection[30,32]. A detection of this reaction would also clearly demonstrate that a neutrino was involved in the scattering.

3.2.2. Exploiting cosmic rays

In the foreseeable future, before the commissioning of the ULHC, target detection of the relic neutrinos has to rely on extremely energetic cosmic rays. Indeed, the resonant annihilation of extremely energetic cosmic neutrinos (EECνs) off relic antineutrinos into Z-bosons (cf. Fig. 7), occuring at the resonance energies

$$ E_{\nu_i}^{\rm res} = \frac{m_Z^2}{2m_{\nu_i}} \simeq 4 \times 10^{21} \left(\frac{\rm eV}{m_{\nu_i}}\right) \ {\rm eV}, \tag{11} $$

offers unique opportunities for relic neutrino detection. On the one hand, one may search for absorption dips[34,35,36,37,11,38,39] in the EECν spectrum at the resonant energies (cf. Fig. 8 (left)), on the other hand, one may look for emission features[40,41,42,43,44,45] (Z-bursts) as protons or photons with energies spanning a decade or more above the predicted Greisen–Zatsepin–Kuzmin (GZK) cutoff[46,47] at $E_{\rm GZK} \simeq 4 \times 10^{19}$ eV (cf. Fig. 8 (right)). This is the energy beyond which the CMB is absorbing

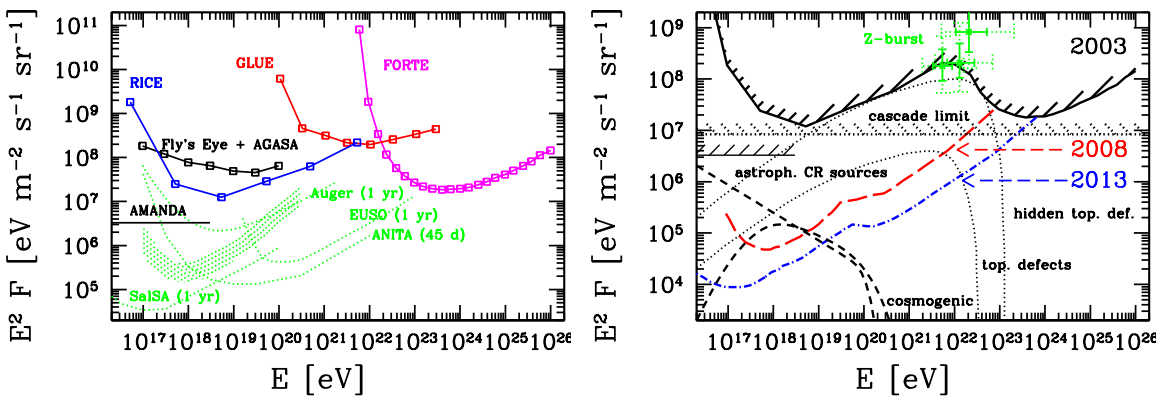

Figure 9: EECν fluxes[11,58,59,60,61,62,63]: current limits and projected sensitivities of dedicated experiments (left), as well as prospects within the next decade (2008 and 2013) and theoretical predictions (right).

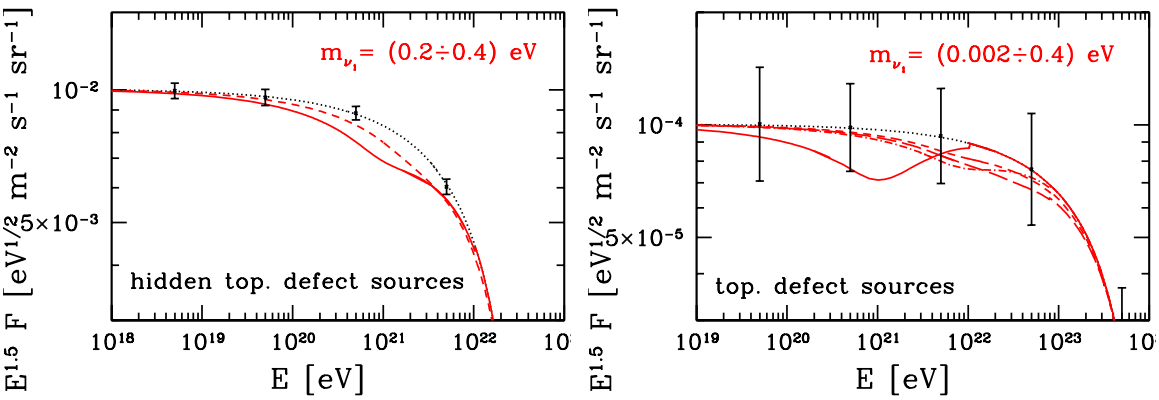

Figure 10: Relic neutrino absorption dips in the EECν flux[11] from hidden topological defect sources (left) and topological defect sources (right), with projected error bars in the year 2013.

to nucleons due to resonant photopion production. Indeed, the association of Z-bursts with the mysterious post-GZK cosmic rays observed[48] by the Akeno Giant Air Shower Array (AGASA) is a controversial[49,50,51] possibility[40,41,42,43,44,45] (cf. Fig. 8 (right)).

Presently planned neutrino detectors (Pierre Auger Observatory[52], IceCube[53], ANITA[54], EUSO[55], OWL[56], and SalSA[57]) operating in the energy regime above 10^{21} eV appear to be sensitive enough to lead us, within the next decade (cf. Fig. 9), into an era of relic neutrino absorption spectroscopy[11,38,39] (cf. Fig. 10), provided that the EECν flux at the resonant energies is close to current observational bounds and the neutrino mass is sufficiently large, $m_\nu \gtrsim 0.1$ eV. In this context it is important to note, that absorption spectroscopy is predominantly sensitive to the relic neutrino background at early times, with the depths of the absorption dips determined largely by the higher number densities at large redshifts ($z \gg 1$) (cf. Fig. 8 (left)). Since

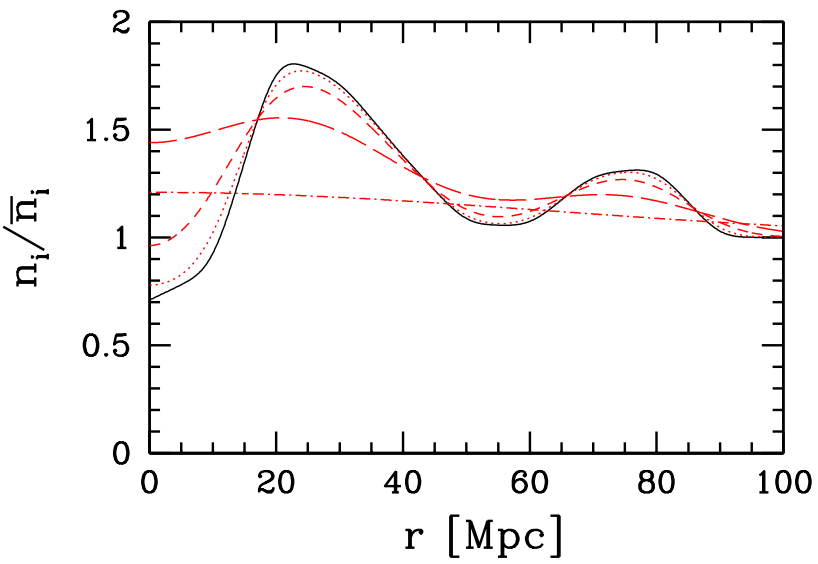

Figure 11: "Large scale" overdensities ($i = \nu, \mathrm{CDM}$) in the local universe[6], with the Milky Way at the origin. The black (solid) line corresponds to the local CDM distribution[44], inferred from peculiar velocity measurements[65], smeared over the surface of a sphere with radius r. The dotted line is the neutrino overdensity for $m_\nu = 0.6$ eV, short dash 0.3 eV, long dash 0.15 eV, and dot-dash 0.04 eV.

neutrinos do not cluster significantly until after $z \lesssim 2$, clustering at recent times can only show up as secondary dips with such minimal widths in energy[64] that they do not seem likely to be resolved by planned observatories.

On the other hand, emission spectroscopy is directly sensitive to the relic neutrino content of the local universe ($z \lesssim 0.01 \Leftrightarrow r_{\mathrm{GZK}} \lesssim 50$ Mpc). However, since the neutrino density contrasts approximately track those of the underlying CDM above the neutrino free-streaming scale, it is clear that there cannot be a substantial neutrino overdensity over the whole GZK volume ($\sim r^3_{\mathrm{GZK}}$). Indeed, the estimated neutrino overdensity in our local GZK zone, with a ~ 5 Mpc smoothing, is always $\lesssim 2$ (cf. Fig. 11). Hence, the overall emission rate cannot be significantly enhanced by gravitational clustering.

Nevertheless, it seems worthwhile to contemplate about "relic neutrino tomography" of the local universe[6,58]. Specifically, one may exploit the fact that there are several galaxy clusters ($\gtrsim 10^{14} M_\odot$), such as Virgo (distance ~ 15 Mpc) and Centaurus (~ 45 Mpc), within the GZK zone (cf. Figure 12) within which we expect significant neutrino clustering (cf. Figure 3). One could then search for directional dependences in the emission events as a signature of EECν annihilating on relic anti-neutrinos (and vice versa)[6]. For example, the angular resolution of AGASA, $\sim 2^\circ$, is already sufficient to resolve the internal structures of, say, the Virgo cluster ($M_{\mathrm{vir}} \sim 10^{15} M_\odot$) which spans some 10° across the sky. Using the N-one-body clustering results in

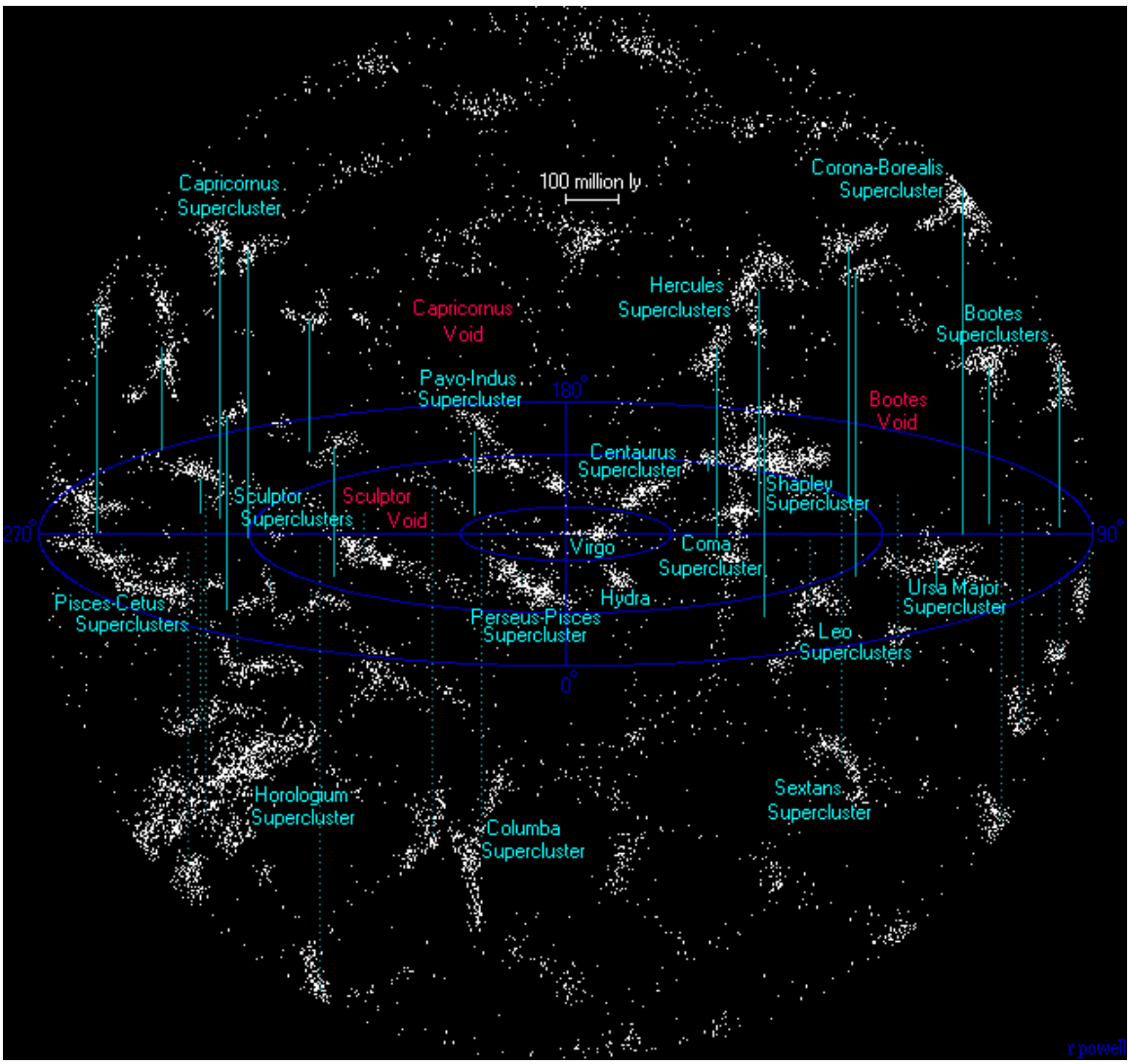

Figure 12: Various massive galaxy superclusters[66] in our "vicinity". The Milky Way is at the center of the coordinate system.

Figure 3, the average neutrino overdensity along the line of sight towards and up to Virgo is estimated to be ~ 45 and ~ 5 for $m_\nu = 0.6$ eV and 0.15 eV respectively, given an angular resolution of $\sim 2°$. The corresponding increases in the number of events coming from the direction of the Virgo cluster relative to the unclustered case, assuming an isotropic distribution of EECν sources, are given roughly by the same numbers, since protons originating from ~ 15 Mpc away arrive at Earth approximately unattenuated. The numbers improve to ~ 55 and ~ 8 respectively with a finer $\sim 1°$ angular resolution. In the most optimistic case of a EECν flux near to the current observational bound (cf. Fig. 9 (right)) and a neutrinos mass $\gtrsim$0.1 eV, EUSO will not only find evidence for the absorption dips, but also for the enhanced

emission from the direction of Virgo due to Z-bursts[58].

4. Conclusions

At present, BBN, CMB, and the large-scale matter power spectrum provide the only observational evidence for the big bang relic neutrinos, at least in the early stages of the cosmological evolution. A more direct, weak interaction based detection of the CνB near the present epoch may proceed in the following chronological order by measuring

i) absorption dips in EECν spectra and Z-bursts in EECR spectra;

ii) macroscopic forces through coherent elastic scattering of relic neutrinos off target material in Cavendish-type torsion balances;

iii) interactions of extremely energetic particles from terrestrial accelerator beams with the relic neutrinos as a target.

Unfortunately, an immediate and guaranteed direct detection does not appear to be feasible. Although the search for signatures of EECν annihilation off the relic neutrinos can start right now, its success entirely rests on the existence of an EECν flux at the resonance energies. The sensitivity of Cavendish-type torsion balances has still to be improved by at least thirteen orders of magnitude for a detectable signal, which postpones this detection techniques probably beyond the year of retirement of the author, $\gtrsim$2025. Finally, an appreciable rate of beam particles with the relic neutrinos requires an Ultimate Large Hadron Collider around the Earth with a beam energy $E_{\rm beam} \gtrsim 10^7$ TeV, which almost certainly will never be built. In the meantime, we can hope to see the late-time relic neutrinos through their gravitational effects in the not-so-large-scale, non-linear part of the matter power spectrum measured by weak gravitational lensing.

5. Acknowledgments

I would like to thank Birgit Eberle, Zoltan Fodor, Sandor Katz, Tom Weiler, and Yvonne Wong for the nice collaboration on different aspects of relic neutrino detection.

6. References

1) For a review:
S. Eidelman *et al.* [Particle Data Group Collaboration], Phys. Lett. B **592** (2004) 1.

2) For a review:
S. Hannestad, New J. Phys. **6** (2004) 108 [arXiv:hep-ph/0404239].
3) S. Pastor, these proceedings.
4) For another recent review:
G. B. Gelmini, talk at *Nobel Symposium 2004: Neutrino Physics*, Haga Slott, Enkoping, Sweden, 19-24 Aug 2004 [arXiv:hep-ph/0412305].
5) S. Singh and C. P. Ma, Phys. Rev. D **67** (2003) 023506 [arXiv:astro-ph/0208419].
6) A. Ringwald and Y. Y. Y. Wong, JCAP **0412** (2004) 005 [arXiv:hep-ph/0408241].
7) C. Lunardini and A. Y. Smirnov, Phys. Rev. D **64** (2001) 073006 [arXiv:hep-ph/0012056].
8) A. D. Dolgov, S. H. Hansen, S. Pastor, S. T. Petcov, G. G. Raffelt and D. V. Semikoz, Nucl. Phys. B **632** (2002) 363 [arXiv:hep-ph/0201287].
9) Y. Y. Y. Wong, Phys. Rev. D **66** (2002) 025015 [arXiv:hep-ph/0203180].
10) K. N. Abazajian, J. F. Beacom and N. F. Bell, Phys. Rev. D **66** (2002) 013008 [arXiv:astro-ph/0203442].
11) B. Eberle, A. Ringwald, L. Song and T. J. Weiler, Phys. Rev. D **70** (2004) 023007 [arXiv:hep-ph/0401203].
12) J. F. Navarro *et al.*, Mon. Not. Roy. Astron. Soc. **349** (2004) 1039 [arXiv:astro-ph/0311231].
13) J. F. Navarro, C. S. Frenk and S. D. M. White, Astrophys. J. **462** (1996) 563 [arXiv:astro-ph/9508025].
14) J. F. Navarro, C. S. Frenk and S. D. M. White, Astrophys. J. **490** (1997) 493.
15) W. Dehnen and J. Binney, Mon. Not. Roy. Astro. Soc. **294** (1998) 429 [arXiv:astro-ph/9612059].
16) A. Klypin, H. Zhao and R. S. Somerville, Astrophys. J. **573** (2002) 597 [arXiv:astro-ph/0110390].
17) Mon. Not. Roy. Astron. Soc. **136** (1967) 101.
18) S. Tremaine and J. E. Gunn, Phys. Rev. Lett. **42** (1979) 407.
19) A. D. Dolgov, these proceedings.
20) K. Abazajian, E. R. Switzer, S. Dodelson, K. Heitmann and S. Habib, Phys. Rev. D **71** (2005) 043507 [arXiv:astro-ph/0411552].
21) S. Hannestad, A. Ringwald, H. Tu and Y. Y. Y. Wong, in preparation.
22) B. F. Shvartsman, V. B. Braginsky, S. S. Gershtein, Y. B. Zeldovich and M. Y. Khlopov, JETP Lett. **36** (1982) 277 [Pisma Zh. Eksp. Teor. Fiz. **36** (1982) 224].
23) P. F. Smith and J. D. Lewin, Phys. Lett. B **127** (1983) 185.
24) G. Duda, G. Gelmini and S. Nussinov, Phys. Rev. D **64** (2001) 122001 [arXiv:hep-ph/0107027].
25) C. Hagmann, in *COSMO98: Proceedings of the Conference on Particle Physics*

and the Early Universe, edited by D. O. Caldwell (AIP, Woodbury NY, 1999), p.460 [AIP Conf. Proc. **478** (1998) 460; arXiv:astro-ph/9902102].
26) C. Hagmann, presented at *American Physical Society (APS) Meeting of the Division of Particles and Fields (DPF 99)*, Los Angeles, USA, 1999, arXiv:astro-ph/9905258.
27) P. F. Smith, in *Trends in Astroparticle Physics*, edited by D. Cline and R. Peccei (World Scientific, Singapore, 1991), p. 311.
28) P. F. Smith, Phil. Trans. Roy. Soc. Lond. A **361** (2003) 2591.
29) B. Müller, in *10th Workshop on Particles and Nuclei: Neutrino Physics*, Heidelberg, Germany, 1987, pp. 269-278.
30) A. C. Melissinos, in *Probing Luminous and Dark Matter*, Rochester, USA, 1999, pp. 262-285.
31) T. J. Weiler, in *Neutrino Telescopes*, Venice, Italy, 2001, vol. 2, pp. 613-636.
32) E. Zavattini, unpublished.
33) Z. Fodor, S. D. Katz and A. Ringwald, prepared for the CERN Cour. **42N5** (2002) 6.
34) T. J. Weiler, Phys. Rev. Lett. **49** (1982) 234.
35) T. J. Weiler, Astrophys. J. **285** (1984) 495.
36) E. Roulet, Phys. Rev. D **47** (1993) 5247.
37) S. Yoshida, H. Y. Dai, C. C. Jui and P. Sommers, Astrophys. J. **479** (1997) 547 [arXiv:astro-ph/9608186].
38) G. Barenboim, O. Mena Requejo and C. Quigg, Phys. Rev. D **71** (2005) 083002 [arXiv:hep-ph/0412122].
39) G. Barenboim, these proceedings.
40) D. Fargion, B. Mele and A. Salis, Astrophys. J. **517** (1999) 725 [arXiv:astro-ph/9710029].
41) T. J. Weiler, Astropart. Phys. **11** (1999) 303 [arXiv:hep-ph/9710431].
42) S. Yoshida, G. Sigl and S. J. Lee, Phys. Rev. Lett. **81** (1998) 5505 [arXiv:hep-ph/9808324].
43) Z. Fodor, S. D. Katz and A. Ringwald, Phys. Rev. Lett. **88** (2002) 171101 [arXiv:hep-ph/0105064].
44) Z. Fodor, S. D. Katz and A. Ringwald, JHEP **0206** (2002) 046 [arXiv:hep-ph/0203198].
45) G. Gelmini, G. Varieschi and T. J. Weiler, Phys. Rev. D **70** (2004) 113005 [arXiv:hep-ph/0404272].
46) K. Greisen, Phys. Rev. Lett. **16** (1966) 748.
47) G. T. Zatsepin and V. A. Kuzmin, JETP Lett. **4** (1966) 78 [Pisma Zh. Eksp. Teor. Fiz. **4** (1966) 114].
48) M. Takeda *et al.*, Phys. Rev. Lett. **81** (1998) 1163 [arXiv:astro-ph/9807193].
49) O. E. Kalashev, V. A. Kuzmin, D. V. Semikoz and G. Sigl, Phys. Rev. D **65** (2002) 103003 [arXiv:hep-ph/0112351].

50) D. S. Gorbunov, P. G. Tinyakov and S. V. Troitsky, Astropart. Phys. **18** (2003) 463 [arXiv:astro-ph/0206385].
51) D. V. Semikoz and G. Sigl, JCAP **0404** (2004) 003 [arXiv:hep-ph/0309328].
52) Pierre Auger Observatory, http://www.auger.org/
53) IceCube, http://icecube.wisc.edu/
54) ANtarctic Impulse Transient Array, http://www.ps.uci.edu/~anita/
55) Extreme Universe Space Observatory, http://www.euso-mission.org/
56) Orbiting Wide-angle Light-collectors, http://owl.gsfc.nasa.gov/
57) Saltdome Shower Array, P. Gorham, D. Saltzberg, A. Odian, D. Williams, D. Besson, G. Frichter and S. Tantawi, Nucl. Instrum. Meth. A **490** (2002) 476 [arXiv:hep-ex/0108027].
58) A. Ringwald, T. J. Weiler and Y. Y. Y. Wong, DESY 05-053, in preparation.
59) V. Berezinsky, these proceedings.
60) F. Halzen, these proceedings.
61) J. G. Learned, these proceedings.
62) D. McKay, these proceedings.
63) T. J. Weiler, these proceedings.
64) T. Reiter, unpublished notes.
65) L. N. da Costa, W. Freudling, G. Wegner, R. Giovanelli, M. P. Haynes and J. J. Salzer, Astrophys. J. Lett. **468** (1996) L5 [arXiv:astro-ph/9606144].
66) www.extrasolar.org